Near threshold three-body final states in ^{7}Li+^{7}Li reactions at E_{lab}=34 MeV

J. A. Liendo
Physics Department, Simon Bolivar University, Caracas, Venezuela

N. Curtis,* D. D. Caussyn, N. R. Fletcher, and T. Kurtukian-Nieto
Department of Physics, Florida State University, Tallahassee, Florida 32306

(Received 4 October 2001; published 4 March 2002)

Reactions of ^{7}Li+^{7}Li at E_{lab}=34 MeV, which lead to charged particle decaying excited states of ^{10}Be, have been studied by use of a detection system sensitive to decay energies of a few hundred keV. The α-particle branching fractions in ^{10}Be*$\rightarrow^4$He+^{6}He have been measured for excited states at E_x=7.542 and ~9.6 MeV. For the 7.542 MeV state an unusually large separation radius is required to explain the observed branching fraction of $\Gamma_\alpha/\Gamma=(3.5\pm1.2)\times10^{-3}$. This result is interpreted in terms of the energy level structure of ^{10}Be as related to analogous states in ^{12}C and to the recent molecular orbital calculations. A new $J^\pi=0^-$ state is observed in the decay ^{10}Be*$\rightarrow^7$Li*(0.478 MeV)+t.

DOI: 10.1103/PhysRevC.65.034317 PACS number(s): 25.70.−z, 23.60.+e, 21.60.Gx, 27.20.+n

I. INTRODUCTION

Charged particle decays of excited states in 1p-shell nuclei often have astrophysical significance when those states are near the decay threshold. Decay energies of a few hundred keV or less are in the region of the stellar Maxwell-Boltzmann distribution where nuclear reaction rates and compound scattering rates compete in light element formation. α-particle decays can also provide cluster structure information for the decaying states. Direct measurements of resonance reactions are extremely difficult at such low energies because of the masking effect of Coulomb scattering. The method used for measuring α-particle decays in the current work is resonant particle decay spectroscopy (RPDS) [1]. Charged particle nuclear reaction fragments are identified in time coincidence in two x-y-position sensitive E-ΔE counter telescopes, determining the particles' masses, charge numbers, kinetic energies, and emission angles. This information provides complete kinematic identification when the reaction is a three-body final state. Conservation of linear momentum is used to determine the energy of the third particle from which an experimentally determined three-body Q-value spectrum is obtained. A well defined peak in the Q-value spectrum identifies the three-body final state reaction of interest. The relative energy between two of the three particles is the decay energy of a resonant state involving that pair when the reaction's final state proceeds by two-body sequential decay. In previous work [2], the method has been used to determine an α-particle decay branching fraction for a 444 keV decay in ^{15}N* and the result agreed with a direct ^{4}He+^{11}B resonance scattering result of Wang *et al.* [3].

The current work reports on near threshold charged particle decays resulting from reactions induced by 34 MeV ^{7}Li ions bombarding ^{7}Li targets at the Florida State University Tandem-LINAC accelerator laboratory. Branching fractions for ^{10}Be* $\rightarrow^4$He+^{6}He have been determined for ^{10}Be excited states at E_x=7.542 and ~9.6 MeV. The branching fraction obtained for the 132 keV decay of the 7.542 MeV state represents the smallest branching fraction ever measured by this method. Although the branching fraction is very small, it represents a large reduced width. This result is used to infer properties of the state relevant to structure models for ^{10}Be. Correspondence with calculated energy level structure also allows reasonable speculation regarding possible J^π assignments and the promise of future experimental results.

II. EXPERIMENTAL METHOD

The details of the RPDS method have been thoroughly explained in our previous publications [2,4]. Here we will only review the detector geometry and other features specific to the current experiment. A schematic velocity addition diagram along with the detector geometry and equations pertinent to the method are shown in Fig. 1. Each of the counter telescopes 1 and 2 consist of ΔE and E detectors of nominal thickness of 67 and 1000 μm, respectively. Each detector has an active area of 12 mm×12 mm which is collimated to 11 mm×11 mm at a distance of 150 mm from the target. The eight-degree detector separation shown in Fig. 1 is a nominal value. The actual separation is a measurement between the centers of position grids placed in front of the detectors during calibration and is accurate to ±0.05°. The angle θ_0 is set at 15°. Although the diagram depicts planar decays, out-of-plane decays are also detected for a limited angular range since the ΔE detectors are position sensitive in the reaction plane shown, while the E detectors measure the position perpendicular to this plane. All nuclear charges and masses Z and A are clearly identified in the counter telescopes up through the beryllium isotopes.

Relative ^{7}Li target thicknesses are determined by use of energy detectors above the exiting beam at angles of 16° and 20°. Energy spectra of 24 MeV ^{16}O particles scattered from the targets can easily separate elastic scattering from the ^{7}Li, ^{12}C, and ^{16}O components of the target. The relative ^{7}Li con-

*Present address: School of Physics and Astronomy, University of Birmingham, Edgbaston, Birmingham B15 2TT, United Kingdom.

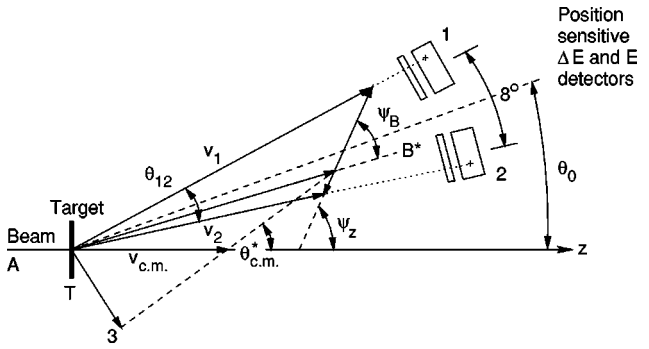

$$A + T \rightarrow B^* + 3, \quad B^* \rightarrow 1 + 2$$

$$E_1 + E_2 + E_3 = E_A + Q_{000}$$

$$E_x(B^*) = E_{rel} + (m_1 + m_2 - m_B)\,c^2$$

$$E_{rel} = \frac{1}{m_1 + m_2}\left[m_1 E_2 + m_2 E_1 - 2\sqrt{m_1 m_2 E_1 E_2}\,\cos\theta_{12}\right]$$

FIG. 1. A velocity addition diagram for three-body final state reactions which proceed by sequential two-body decays, equations for the process, and a schematic of detector placements.

tent of targets is essential to determining relative two-body and three-body final state cross sections needed for branching-fraction determinations. A secondary gold target and silicon detector, located approximately 40 cm downstream from the primary target, are used to make direct measurement of the beam energy loss in the primary target. Target oxidation and carbon buildup are thereby continuously monitored. The ^{7}Li targets used corresponded to about 200 keV energy loss to the incident beam.

III. EXPERIMENTAL RESULTS

Coincidence data were collected for five days with a 6 nA beam of $^7Li^{+3}$ ions. Since detected nuclei are identified uniquely, a variety of states corresponding to different excited nuclei and fragment pairs can be investigated. Shown in Fig. 2 are E_{tot} spectra ($E_{tot}=E_1+E_2+E_3=Q+E_A$) for detected fragment pairs of (a) $\alpha+\alpha$, (b) $\alpha+^6$He, and (c) ^{7}Li$+t$. In Figs.. 2(a) and 2(b) the peaks near 41 MeV represent a three body final state of $2\alpha+^6$He with all particles in their ground states. Several other peaks appear in Fig. 2(a) corresponding to the undetected particle in excited states. The ^{6}He produced in the first excited state is, of course, from the ^{7}Li content in the target, while several excited states of ^{11}B appear from the ^{12}C content in the formvar target backing and from carbon buildup on the target during the experiment. In Fig. 2(c), the detected pair is $^7Li_{g.s.}+t$. The first excited state of ^{7}Li appears in the E_{tot} spectrum since ^{7}Li* γ decays, but it is detected as $^7Li_{g.s.}$ with the introduction of very little change in the emission angle and kinetic energy of the originally emitted ^{7}Li*. This is discussed later in the context of ^{10}Be*$\rightarrow^7$Li$+t$ decays.

If we select those events in Fig. 2(a), which have ^{6}He in the ground state, then the relative energy between the two detected particles will yield a decay energy spectrum for

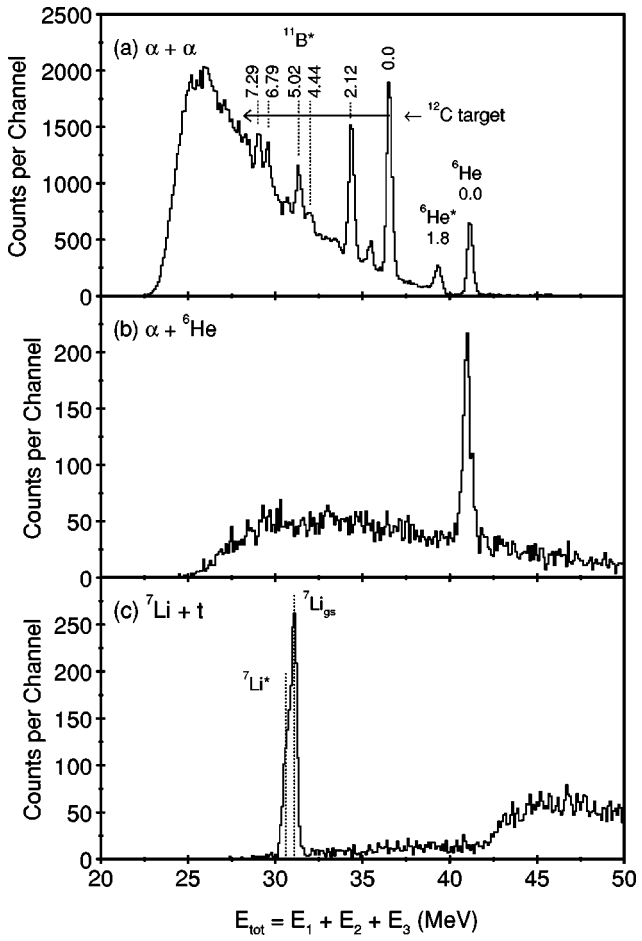

FIG. 2. Experimental Q-value spectra for coincidence pairs of (a) $\alpha+\alpha$, (b) $\alpha+^6$He, and (c) ^{7}Li$+t$. The actual Q value is given approximately by $E_{tot}-34$ MeV.

$^8Be_{g.s.}$. Such a spectrum is shown in Fig. 3. The decay energy resolution in Fig. 3 is significantly worse in the present experiment than in earlier work [4], which employed lower count rates and radioactive source calibration energies. With

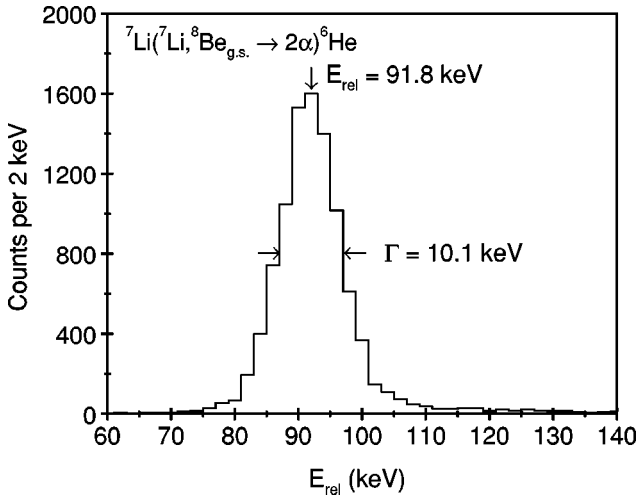

FIG. 3. Decay energy spectrum for the breakup of $^8Be_{g.s.}$, showing the calibration and resolution observed in this experiment.

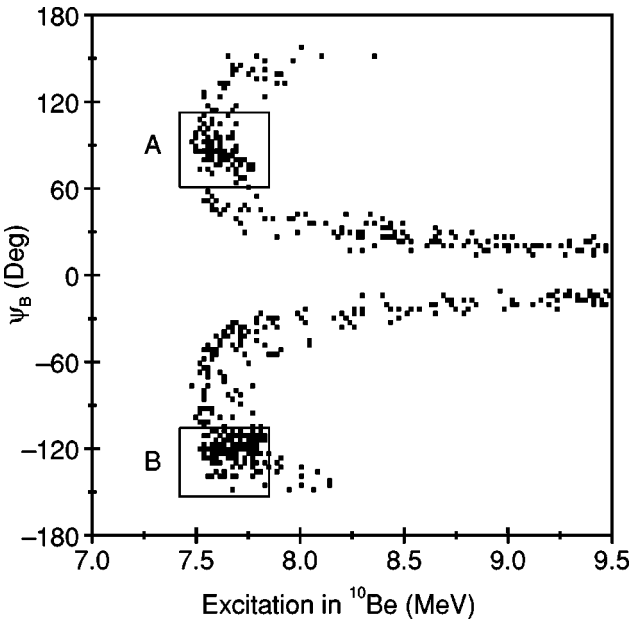

FIG. 4. Event plot of the relative energy between detected particles α and ^{6}He vs the angle between their decay axis and the emission direction of the excited ^{10}Be nucleus. The decay threshold energy 7.410 MeV has been added to the horizontal axis to convert it to excitation energy in ^{10}Be. The regions A and B are dominated by the reaction ^{7}Li(^{7}Li,^{8}Be*)^{6}He.

the large number of events in Fig. 3 we can observe the effects of detector energy resolution and position resolution independently by selecting different ranges in decay angle, Ψ_B. From this information we deduce an expected decay-energy resolution for ^{10}Be*(7.542 MeV) of 12 to 13 keV. Since the energy width of the 7.542 MeV state is (6.3 $\pm$0.8) keV [5], we would expect to observe the α-particle decay of the 7.542 MeV state with an energy resolution of 15 keV or less. At greatly decreased detection efficiency, the state in ^{10}Be near E_x=9.6 MeV can be observed at an estimated energy resolution of about 60 to 80 keV.

A. α-particle decay and the branching fraction Γ_α/Γ

To observe the decays ^{10}Be*$\rightarrow{}^4$He+^{6}He we select those events in the peak near $E_{\rm tot}$=41 MeV in Fig. 2(b). The excitation energy spectrum for ^{10}Be* decays is encumbered by partial detection of the reaction ^{7}Li+^{7}Li$\rightarrow{}^8$Be*+^{6}He in which we detect the ^{6}He in coincidence with one of the decay α particles from ^{8}Be*. This problem is illustrated in Fig. 4 showing an event plot of Ψ_B vs excitation energy in ^{10}Be ($E_x=E_{\rm rel}+E_{\rm th}$). The clusters of events in regions A and B are primarily due to ^{8}Be* decay from an excitation of 7 to 10 MeV. The negative values of Ψ_B correspond to detecting the alpha particle in detector 1 and the ^{6}He in detector 2. For the ^{8}Be-decay events in region B of Fig. 4, this leads to a smaller production angle for the excited ^{8}Be and it also leads to a ^{8}Be-decay energy closer to the center of the broad $J^\pi=4^+$ state at $\sim$11 MeV. Each of these effects generate a greater intensity of detected ^{8}Be decay, which is evident in region B of Fig. 4. Region B of Fig. 4 covers a range

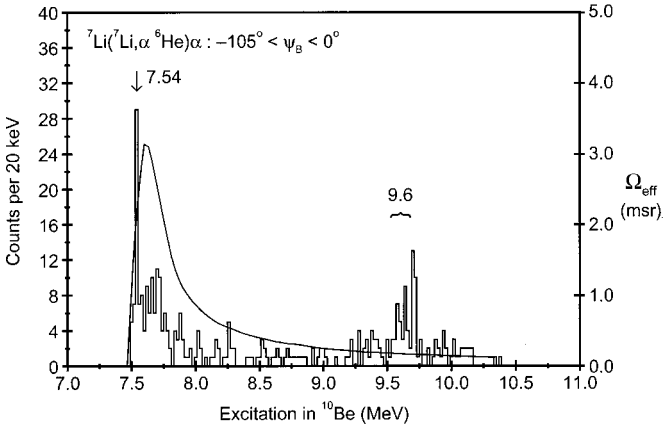

FIG. 5. Excitations in ^{10}Be as calculated for each event as $E_{\rm rel}+E_{\rm th}$ for the reaction ^{7}Li+^{7}Li$\rightarrow{}^4$He+^{6}He+^{4}He. The smooth curve represents the total effective solid angle $\Omega_{\rm eff}$ (msr) for the detection of ^{10}Be* decays as calculated by a Monte Carlo simulation. For this restricted range of Ψ_B, the effective solid angle at E_x=7.542 MeV is (0.79$\pm$0.01) msr. The natural width of the 9.6 MeV state is 141$\pm$10 keV [7].

in $|\Psi_B|$ which is shifted to larger values from those of region A, leaving a larger angular range for the unobscured observation of ^{10}Be*(7.542 MeV).

The yield of ^{10}Be*$\rightarrow{}^4$He+^{6}He decay events is plotted in Fig. 5 vs excitation energy in ^{10}Be for the decay angular range $-105°<\Psi_B<0°$. The smooth curve and the scale on the right of the figure represent the total effective solid angle for detection of ^{10}Be*$\rightarrow{}^4$He+^{6}He decay as determined by use of the Monte Carlo code BEAST [6]. It appears that some of the background due to ^{8}Be* decay still remains in the region of E_x=7.5 to 7.8 MeV, however, a significant yield in a single channel (20 keV/channel) clearly indicates α-particle decay of the 7.542 MeV state of ^{10}Be. The expected observable energy resolution at this excitation is less than 15 keV. Decay energy calibration and resolution are excellent near threshold, since there they depend primarily on position resolution of the detectors. At excitation near 9.6 MeV, where position resolution has little effect, both the accuracy of the energy calibration and resolution deteriorate. For this reason we do not regard the apparent yield near 9.7 MeV, which persists in a spectrum ungated in Ψ_B, as a separate state.

The branching fraction for α-particle decay of the 7.542 MeV state depends on the yield extracted from Fig. 5 (22 $\pm$6 events), and the yield from a similar spectrum for $0°<\Psi_B<105°$ (14$\pm$8 events) where the ^{8}Be background is higher by nearly a factor of 3. A combination of these two yields, which correspond to different ranges of the correlation angle Ψ_z, is used as the term N_λ in Eqs. (3.2) and (3.3) below. In the reaction ^{7}Li(^{7}Li,α)^{10}Be*(λ), resulting in the formation of ^{10}Be in the excited state λ, the differential cross section in the center of mass can be written in terms of a constant K and the number of α particles detected in the two-body reaction N_α as

$$d\sigma(\theta_{\rm c.m.})/d\Omega = KN_\alpha/[Q_\alpha T_\alpha \Delta\Omega_\alpha({\rm c.m.})]. \qquad (3.1)$$

This can also be written in terms of the number, N_λ, of excited ^{10}Be nuclei detected by their subsequent two-body decay $\lambda \rightarrow \alpha + {}^6$He as

$$d\sigma(\theta_{\text{c.m.}})/d\Omega = KN_\lambda(\Gamma/\Gamma_\alpha)/[Q_\lambda T_\lambda \Delta\Omega_\lambda(\text{c.m.})]. \tag{3.2}$$

Equating these cross section equations gives an expression for the branching fraction:

$$\Gamma_\alpha/\Gamma = \{N_\lambda/N_\alpha\}(Q_\alpha/Q_\lambda)(T_\alpha/T_\lambda) \times[\Delta\Omega_\alpha(\text{c.m.})/\Delta\Omega_\lambda(\text{c.m.})]. \tag{3.3}$$

The ratio Q_α/Q_λ is the ratio of beam charge collected in the two-body and three-body measurements, while T_α/T_λ is the ratio of target thicknesses as determined by the ^{16}O scattering into the out of plane detectors. The solid angle for the three-body reaction $\Delta\Omega_\lambda$(c.m.) is calculated by a Monte Carlo code for the appropriate angular ranges in Ψ_B. For the negative values of Ψ_B, the weighted mean value of θ_λ(c.m.) is $\sim$33.13°, as determined in the Monte Carlo calculation, corresponding to $\theta_\lambda(\text{lab}) = 14.2°$. Since for $\Psi_B < 0$, $\theta_\alpha > \theta_{^6\text{He}}$, the ^{10}Be* angle is always less than $\theta_0 = 15°$. Since the reactions involve two identical particles in the initial state, the cross sections are symmetric about $\theta(\text{c.m.}) = 90°$, therefore both the α particle and ^{10}Be yields can be determined at forward angles in the laboratory. The corresponding laboratory angle for the two-body reaction is 21.8°, and the yield of α particles is an interpolated value between measurements at 20° and 25°. Similar determinations are made for yields for positive values of Ψ_B.

The resulting branching fraction for the state at $E_x = 7.542$ MeV is $\Gamma_\alpha/\Gamma = (3.5 \pm 1.2) \times 10^{-3}$. A similar application to the yield near $E_x = 9.6$ MeV gives $\Gamma_\alpha/\Gamma = (0.16 \pm 0.04)$. In both cases the majority of the quoted uncertainty is from the poor yield in the three-body reaction. There is an inherent error in this application of Eq. (3.3). The yields divided by the effective solid angles $N_\lambda/d\Omega_\lambda$(c.m.) do not represent an exact average value over the entire angular correlation angle Ψ_z. In the case of decay of the state at 7.542 MeV, $J^\pi = 2^+$, the angular correlation would be of the form of Eq. (3) of Ref. [7], with considerable $m = 1$ contribution due to the nonzero production angle of ^{10}Be*, in addition to the $m = 1$ contribution due to nonzero J values in the initial state [7]. The effect would be to reduce the anisotropy in the angular correlation function. Since the yield is extracted over nearly a 100° range in $|\Psi_z|$, we expect the error introduced to be significantly less than the 35% uncertainty already quoted in the branching fraction. For the decay of the excitation near 9.6 MeV, our detector geometry samples only very limited regions of the correlation angle $|\Psi_z|$ and therefore that branching fraction might easily have an uncertainty twice the value of the quoted known uncertainties.

B. ^{10}Be$\rightarrow{}^7$Li$+t$ decay near $E_x = 18$ MeV

The decay threshold for ^{10}Be*$\rightarrow{}^7$Li$+t$ is at $E_x \cong 17.25$ MeV. States at $E_x = 17.79$ and 18.55 MeV have been observed prominently in the ^{7}Li(t,n) resonance reaction [5]. We have attempted to observe these and possibly other states in ^{7}Li$+t$ decay of ^{10}Be* formed in the ^{7}Li $+{}^7$Li reaction at $E(\text{lab}) = 34$ MeV. The Q spectrum of Fig. 2(c) has been expanded and described by Gaussian line shapes and the result is shown in Fig. 6. Restricting the widths of the two Gaussian line shapes to be the same, we obtain a Q-value resolution of (408 ± 11) keV and peak separations of $\Delta Q = (470 \pm 14)$ keV. Since the first excited state of ^{7}Li is at 478 keV, the lower energy peak can clearly be identified as coming from the three-body final state of ^{7}Li*$+t+\alpha$. Of course the ^{7}Li* is detected as ^{7}Li$_{\text{g.s.}}$ following γ decay. The emission of a γ ray causes only a $\pm 0.05°$ spread in the ^{7}Li-emission angle and about ± 40 keV in energy spread. These values will have very little effect on decay energy calculations or on the observed widths.

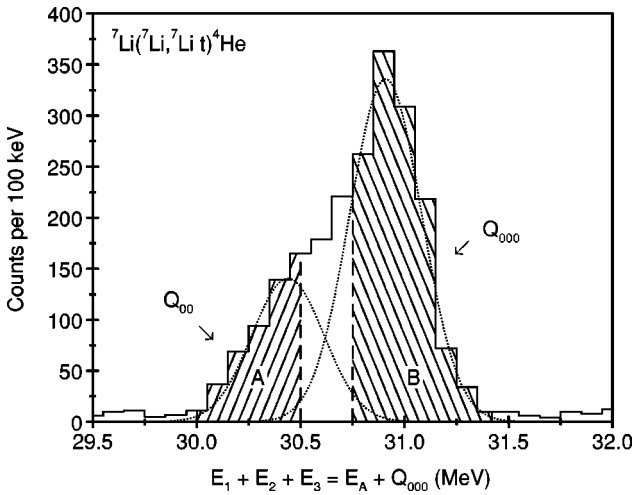

FIG. 6. Expanded Q spectrum from Fig. 2(c) for the reactions ^{7}Li(^{7}Li,^{7}Li$_{\text{g.s.}}t)\alpha$ and ^{7}Li(^{7}Li,^{7}Li*$t)\alpha$. Regions A and B are used for producing the decay energy spectra of Fig. 7.

In an attempt to isolate the ^{7}Li*$+t$ and ^{7}Li$_{\text{g.s.}}+t$ decays, we have formed the excitation spectra for ^{10}Be by gating on regions A and B of Fig. 6. These spectra are displayed as Figs. 7(a) and 7(b), respectively. The effective solid angle for detection of the ^{7}Li$+t$ decay has a decay-energy dependence very similar to that shown in Fig. 5, with a maximum effective solid angle of $\sim$4.3 msr at $E_x \sim 17.4$ MeV and falling to one tenth the maximum value about 800 keV higher in excitation. The effective solid angle for detection of ^{7}Li*$+t$ is nearly identical but shifted to higher energy by the excitation energy of the first excited state of ^{7}Li. The peaks identified at $E_x = 17.76$ and 18.5 MeV have observed widths of about 140 and 320 keV, respectively. The energy resolution is expected to vary from about 20 keV near detection threshold to about 60 keV at the high energy cutoff. These states are clearly identified with the known [5] states at $E_x = 17.79$ and 18.55 MeV since our extracted widths are consistent with currently accepted values of (110 ± 35) and $\sim$350 keV respectively. Our energy calibration differences might arise from detecting high energy Li ions and tritons, while calibrating with He ions. An apparent new state is observed in the ^{10}Be*$\rightarrow{}^7$Li*$+t$ decay at an indicated excitation of 18.11 MeV. Accepting the known excitation ener-

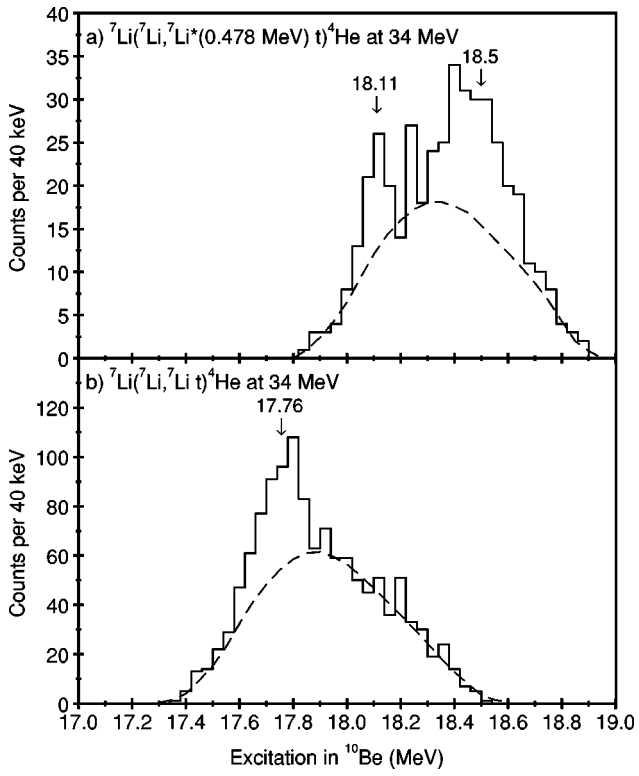

FIG. 7. Excitation energy in ^{10}Be as calculated for $^7\mathrm{Li}^* + t$ decays (a), and for $^7\mathrm{Li}_{\mathrm{g.s.}} + t$ decays (b). The continuum background from a direct three-body final state should be virtually the same for either decay branch, as shown approximately by dashed lines. The new excited state at 18.11 MeV has a calibration corrected energy of (18.15 ± 0.05) MeV (see text).

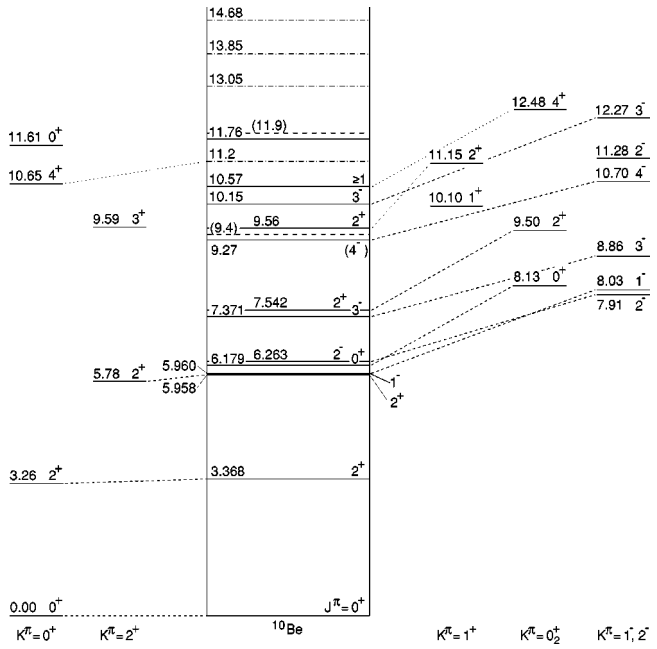

FIG. 8. Energy level diagram for ^{10}Be for excitations below 15 MeV, showing excitation energies and known J^π values. The levels indicated by dot-dash lines require further verification [7,10]. The excitation energies in parentheses are less certain. The columns identified by K^π values are the results of a molecular orbital calculation [11]. Associations between calculated and experimental energy levels are indicated by connecting dashed lines. Connecting dotted lines are speculative assignments (see text). The calculation for $K^\pi = 0^+$, $J^\pi = 0^+$ state has been energy normalized to the ^{10}Be ground state.

gies of 17.79 and 18.55 MeV [5], a corrected energy calibration places this new excited state at $E_x = (18.15 \pm 0.05)$ MeV with a width of $\Gamma = (100 \pm 30)$ keV. The absence of any yield from this state in Fig. 7(b) is discussed in Sec. IV. The single channel excess yield in Fig. 7(a) at 18.24 MeV could be a few events from the 17.76 MeV peak being included in the *A* gate of Fig. 6.

IV. DISCUSSION AND CONCLUSIONS

Experiments completed in the last few years have greatly expanded our knowledge of the energy level structure of ^{10}Be [7–10]. These and earlier works, discussed in detail in Ref. [7], result in the energy level diagram illustrated in Fig. 8 showing known excitations below 15 MeV. The four highest energy states have been observed in two experiments [7,10] with poor statistics, so they require further verification. Also in the figure are the results of recent molecular orbital calculations for the energy level structure of ^{10}Be as identified by the K^π bands. Dashed lines connecting calculated and experimental energy levels indicate the corresponding states [11]. This diagram provides the framework for the following discussion of branching fractions.

A discussion of the branching fractions determined in this work is facilitated by converting them to reduced widths, because of the strong inhibiting effect of the Coulomb barrier on α-particle decay near threshold. The experimentally determined reduced widths are given by Lane and Thomas [12] as $(\gamma_\alpha)^2 = \Gamma_\alpha/(2P_l)$, where the α-particle width Γ_α is the natural width of the state Γ [5] times the measured branching fraction. We use unpublished tables [13] for the penetrability functions P_l, where the l value for the decay is $l = 2$ for both $E_x = 7.542$ and ~ 9.6 MeV. The experimental reduced widths can be compared with the single particle reduced widths also given by Lane and Thomas as $(\gamma^{\mathrm{SP}})^2 = \hbar^2/(\mu_\alpha r^2)$. The ratio $(\gamma_\alpha)^2/(\gamma^{\mathrm{SP}})^2$ would be expected to have a maximum value equal to the number of α-particle clusters in the decaying state, in this case two. Setting this ratio equal to two for the 7.542 MeV state leads to a channel radius for its decay of $r_c \sim (8 \pm 1)$ fm. Smaller radii require even larger ratios of the reduced widths. For the decay of the state at $E_x \sim 9.6$ MeV, the ratio of the experimental reduced width to single particle reduced width is only a few percent (6 to 2 %) for channel radii of 3 to 8 fm. These values indicate vastly different structures for these two $J^\pi = 2^+$ states.

In previous work the close correspondence in the excitation energies of cluster states in ^{12}C and ^{10}Be has been noted [7]. Excitation energies of states in ^{10}Be are very nearly given by multiplying ^{12}C excitation energies by the mass ratio (10/12) for the low lying excited ^{12}C-cluster states with $J^\pi = 2^+$, 0^+, and 3^-. The first excited 0^+ state in ^{12}C is known to resemble a linear chain of α particles. The corresponding $J^\pi = 0^+$ state in ^{10}Be is at $E_x = 6.179$ MeV. In the description of Itagaki [11], this state is the band head for the

$K^\pi=0_2^+$ band. The $J^\pi=2^+$ band member is the 7.542 MeV state for which we have measured the α-decay branching fraction. In analogy with the ^{12}C structures, if we assume the ^{10}Be bands of $K^\pi=0^+$ and 0_2^+ have triangular and linear arrangements, respectively, of the α-2n-α clusters, then using the energy-level spacings in these bands one can show that the α-^{6}He separation is nearly twice ($\sim$1.88) as large for the $K^\pi=0_2^+$ band as it is in the $K^\pi=0^+$ band. The very large separation radius required by our branching fraction measurement therefore supports the assignment of Itagaki [11] of the $E_x=7.542$ MeV state to the $K^\pi=0_2^+$ band.

All ^{10}Be excitations shown in Fig. 8 for $E_x>9.5$ MeV have been observed in α-particle decay [7,9,10] and therefore must have natural parity. The calculated bands with $K^\pi=0^+$ and $K^\pi=0_2^+$ are nearly perfect rotors, $E_J-E_0=J(J+1)\hbar^2/2I$. We can therefore speculate as to the location of $J^\pi=4^+$ states from the known excitation energies of the $J^\pi=0^+$ and 2^+ states in these bands. The result is associating the $E_x=11.2$ MeV state with the 4^+ state of the $K^\pi=0^+$ band, and the $E_x=10.57$ MeV state with the 4^+ state of the $K^\pi=0_2^+$ band. An earlier speculation had placed the first 4^+ state at 11.76 MeV [8]. A measurement of the α-particle decay angular correlations for these three excited states ($E_x=10.57$, 11.2, and 11.76 MeV) could determine which if any are the missing 4^+ states. Determination of the reduced widths by this method could also possibly distinguish between the two K-band assignments because of the large difference in the α-^{6}He channel radius required in these bands. Obviously a reaction for populating these states more abundantly than the current one must be found to make these measurements.

The existence of a new state at an excitation of (18.15 ± 0.05) MeV (see Fig. 7 and its caption) presents an interesting situation, since it is observed in ^{7}Li*$+t$ decay and not in the ^{7}Li$_{g.s.}+t$ decay. The reason for this may be due to different allowed l values for the decay and the different J^π values of ^{7}Li in its ground state and first excited state. Using Eq. (3.2) and the expressions for the reduced widths for the two decay channels $\lambda\rightarrow{}^7\mathrm{Li}+t$ and $\lambda^*\rightarrow{}^7\mathrm{Li}^*+t$, the expected number of detected decays N_λ involving the ground state of ^{7}Li can be expressed as

$$N_\lambda=N_\lambda^*[(\gamma_\lambda)^2/(\gamma_\lambda^*)^2](\Delta\Omega_\lambda/\Delta\Omega_\lambda^*)(P_l/P_l^*)(f_B/f_A). \tag{4.1}$$

The number of decays of $\lambda^*\rightarrow{}^7\mathrm{Li}^*+t$ as determined from Fig. 7(a) is N_λ^*. The ratio of effective solid angles for detection in the two decay branches has a value of 0.40. The ratio of reduced widths must be very nearly one, since both ^{7}Li and ^{7}Li* have unit spectroscopic factors for $\alpha+t$ clustering [14]. The factor (f_B/f_A) is the ratio of the fractions of the full Gaussians accepted in the gates A and B shown in Fig. 6. The calculated values of N_λ are given in Table I for different assumed values of J^π for the ^{10}Be state at 18.15 MeV excitation. The penetrabilities P_l and P_l^*, are for the minimum allowed l values and for a channel radius of $r_c=r_0(A_1^{1/3}+A_2^{1/3})$ with $r_0=1.5$ fm. Comparing the results in Table I with the data in Fig. 7(b), we can firmly conclude that $J^\pi\leqslant1^-,2^+$, but most probably $J^\pi=0^-$. This state has not been observed in ^{7}Li$+t$ resonance work [5]. This could be because of lacking the required $l=2$ strength for $J^\pi=0^-$ at low bombarding energy. The states at $E_x=17.79$ and 18.55 MeV have been observed in the ^{7}Li(t,n) resonance reaction. With tentative J^π assignments of 2^- [5], the resonances can be reached by $l=0$. The fact that a state at $E_x=18.15$ MeV could also be formed by $l=0$ if it had $J^\pi=1^-$, but it is not observed in ^{7}Li(t,n), argues against that assignment for the new state and in favor of $J^\pi=0^-$.

TABLE I. Calculated yield N_λ for ^{10}Be*(18.15 MeV)$\rightarrow{}^7\mathrm{Li}_{g.s.}+t$ vs assumed J^π of the decaying state indicating a $J^\pi=0^-$ assignment.

J^π	$l^*_{\min}$	$l_{\min}$	(P_l/P_l^*)	N_λ
0^+, 1^+, 2^+	1	1	1.81	33
0^-	0	2	0.40	7
1^-	0	0	1.57	29
2^-	2	0	12.5	$\sim$220
3^-	2	2	3.19	58
3^+	3	1	45	$\sim$800

To summarize, we have measured branching fractions for the decay of ^{10}Be* at excitations of 7.542 and $\sim$9.6 MeV into ^{4}He$+^6$He. The results clearly associate the 7.542 MeV state with the $K^\pi=0_2^+$ band of Itagaki [11]. Because of the close correspondence of the $K^\pi=0^+$ and 0_2^+ bands to simple rotations, we speculate that the first $J^\pi=4^+$ state is at $E_x=10.57$ MeV, associated with the $K^\pi=0_2^+$ band, and the second 4^+ state is at $E_x=11.2$ MeV, associated with the $K^\pi=0^+$ band. We have also determined a new $J^\pi=0^-$ state in the decay branch $^{10}\mathrm{Be}^*\rightarrow{}^7\mathrm{Li}^*+t$, at $E_x=(18.15\pm0.05)$ MeV with a total width of $\Gamma=(100\pm30)$ keV. Extension of a molecular orbital model similar to Ref. [11] would prove useful in explaining the new states in ^{10}Be with excitations above 11.2 MeV.

ACKNOWLEDGMENTS

We would like to thank Mr. Powell Barber and the entire graduate student and technical staff for their help during the preparation and data acquisition phases of this experiment. We also acknowledge the many helpful discussions with Professor D. Robson regarding the analysis and interpretation of these data. Discussions with Professor Kirby Kemper are also gratefully acknowledged. This work was supported in part by the National Science Foundation under Grant No. PHY-9523974.

[1] W.D.M. Rae and R.K. Bhomik, Nucl. Phys. **A420**, 320 (1984); R.K. Bhomik and W.D.M. Rae, Phys. Lett. **136B**, 149 (1984); S. Marsh and W.D.M. Rae, *ibid.* **153B**, 21 (1985).
[2] J.A. Liendo, N.R. Fletcher, E.E. Towers, and D.D. Caussyn, Phys. Rev. C **51**, 701 (1995).
[3] T.R. Wang, R.B. Vogelaar, and R.W. Kavanagh, Phys. Rev. C **47**, 682 (1991).
[4] N.R. Fletcher, M.B. Hopson, C. Lee, M.A. Tiede, Z. Yang, and J. Liendo, Nucl. Instrum. Methods Phys. Res. A **372**, 439 (1996).
[5] F. Ajzenberg-Selove, Nucl. Phys. **A490**, 1 (1988).
[6] D.D. Caussyn, G.L. Gentry, J.A. Liendo, N.R. Fletcher, and J.F. Mateja, Phys. Rev. C **43**, 205 (1991).
[7] N. Curtis, D.D. Caussyn, N.R. Fletcher, F. Maréchal, N. Fay, and D. Robson, Phys. Rev. C **64**, 044604 (2001).
[8] S. Hamada, M. Yasue, S. Kubono, M.H. Tanaka, and R.J. Peterson, Phys. Rev. C **49**, 3192 (1994).
[9] N. Soić, S. Blagus, M. Bogovac, S. Fazinić, M. Lattuada, M. Milin, D. Miljanić, D. Rendić, C. Spitaleri, T. Tadić, and M. Zadro, Europhys. Lett. **34**, 7 (1996).
[10] M. Freer, J.C. Angélique, L. Axelsson, B. Benoit, U. Bergmann, W.N. Catford, S.P.G. Chappell, N.M. Clarke, N. Curtis, A. D'Arrigo, E. de Goes Brennard, O. Dorvaux, B.R. Fulton, G. Giardina, C. Gregori, S. Grévy, F. Hanappe, G. Kelly, M. Labiche, C. Le Brun, S. Leenhardt, M. Lewitowicz, K. Markenroth, F.M. Marqués, M. Motta, J.T. Murgatroyd, T. Nilsson, A. Ninane, N.A. Orr, I. Piqueras, M.G. Saint Laurent, S.M. Singer, O. Sorlin, L. Stuttgé, and D.L. Watson, Phys. Rev. C **63**, 034301 (2001).
[11] N. Itagaki and S. Okabe, Phys. Rev. C **61**, 044306 (2000); N. Itagaki (private communication).
[12] A.M. Lane and R.G. Thomas, Rev. Mod. Phys. **30**, 257 (1958).
[13] W.J. Thompson, Florida State University internal report, 1965 (unpublished).
[14] K.W. Kemper (private communication).